Journal of the Korean Geo-Environmental Society
17(4): 17～31. (April, 2016) http://www.kges.or.kr
ISSN 1598-0820
DOI http://dx.doi.org/10.14481/jkges.2016.17.4.17

Shallow Landslide Assessment Considering the Influence of Vegetation Cover

Tran The Viet[1] · Giha Lee[†] · Minseok Kim[2]

Received: January 4th, 2016; Revised: January 5th, 2016; Accepted: March 14th, 2016

ABSTRACT : Many researchers have evaluated the influence of vegetation cover on slope stability. However, due to the extensive variety of site conditions and vegetation types, different studies have often provided inconsistent results, especially when evaluating in different regions. Therefore, additional studies need to be conducted to identify the positive impacts of vegetation cover for slope stabilization. This study used the Transient Rainfall Infiltration and Grid-based Regional Slope-stability Model (TRIGRS) to predict the occurrence of landslides in a watershed in Jinbu-Myeon, Pyeongchang-gun, Korea. The influence of vegetation cover was assessed by spatially and temporally comparing the predicted landslides corresponding to multiple trials of cohesion values (which include the role of root cohesion) and real observed landslide scars to back-calculate the contribution of vegetation cover to slope stabilization. The lower bound of cohesion was defined based on the fact that there are no unstable cells in the raster stability map at initial conditions, and the modified success rate was used to evaluate the model performance. In the next step, the most reliable value representing the contribution of vegetation cover in the study area was applied for landslide assessment. The analyzed results showed that the role of vegetation cover could be replaced by increasing the soil cohesion by 3.8 kPa. Without considering the influence of vegetation cover, a large area of the studied watershed is unconditionally unstable in the initial condition. However, when tree root cohesion is taken into account, the model produces more realistic results with about 76.7% of observed unstable cells and 78.6% of observed stable cells being well predicted.

Keywords : Stability, Vegetation cover, Landslide scars, Root cohesion, Back-calculation

1. Introduction

The increasing trend of landslides in mountainous and hilly areas of Korea in recent decades has set off an alarm for researchers to find more reliable methods for landslide early warning and prediction. However, analyzing the stability of natural forested slopes has never been an easy task because it depends on numerous factors those related to the effects of vegetation such as the influence of trees on soil reinforcement, soil moisture distribution and the amount of rainwater reaching the ground. However, many assumptions, especially the hypothesis of ignoring the role of vegetation cover in slope stabilization, are still needed to identify the remaining unknown variables.

Tree roots are considered to be a major contributor to soil strength and slope stability (O'Loughlin, 1974; O'Loughlin & Ziemer, 1982; Abe & Ziemer, 1991; Ali & Osman, 2008; Kim et al., 2010b; Lee et al., 2012b; Kim et al., 2013). However, assessment of this contribution remains an unsolved problem (Frank et al., 2009). An analysis of aerial photographs of landslides in Pyeongchang, Korea during 2006 by the Korea Forest Research Institute (KFRI) demonstrated that landslides occurred six times more frequently in logged areas and monoculture forests than in mixed or natural forests (Kim et al., 2010b). Additionally, landslide frequency and area have been reported to increase drastically in the 3～10 years following logging (O'Loughlin & Ziemer, 1982). Another study by Swanston & Marion (1991) pointed out a 3.5 times greater landslide rate in harvested areas than in unharvested areas over approximately 20 years in Southeast Alaska. Also, the frequency of landslides in logged areas was found to be nine times higher than that in unlocked forest areas around Vancouver Island, BC, Canada (Jakob, 2000).

Trees have significant effects on shallow landslide development in steep, forested watersheds during severe storm events (Kim et al., 2013; Schwarz et al., 2013). Landslide scars often reveal broken roots tendrils, suggesting that the tensile strength of the roots was mobilized during failure (Schmidt

1) Department of Construction and Disaster Prevention Engineering, Kyungpook National University
Division of Geotechnical Engineering., Thuyloi University
† Department of Construction and Disaster Prevention Engineering, Kyungpook National University (Corresponding Author : leegiha@knu.ac.kr)
2) International Water Resources Research Institute, Chungnam National University

et al., 2001). Presumably, root systems contribute significantly to the stability of many forested slopes by binding the soil mass and by helping to anchor the soil mantle to the sub-stratum (O'Loughlin, 1974). Tree roots are known to reinforce soil by increasing soil shear strength. However, few studies have quantified soil reinforcement by tree roots because of some experimental difficulties (Kim et al., 2010b). Quantitatively analyzing the soil reinforcement caused by roots has many difficulties because root structures are easy to be destroyed during the assessment.

In short-term assessment, O'Loughlin (1974) stated that vegetation often affects the stability of slopes primarily in two ways: (1) by removing soil moisture and reducing soil pore water pressure through evapotranspiration and (2) by mechanically reinforcing the soil with tree roots and increasing the surcharge on the slope soil mantle. Mechanical effects, such as root reinforcement, act directly whereas hydrological effects, such as water uptake, act indirectly (Kim et al., 2010b). Among the two, the latter factor is not particularly important for shallow landslides that occur during an extended rainy season (Sidle & Ochiai, 2006). Therefore, the rainfall interception model was not employed in this study because rainfall interception has little impact on landslide initiation during the short duration of a single rainfall event (Kim et al., 2013).

This study applied Transient Rainfall Infiltration and Grid-based Regional Slope-stability analysis (TRIGRS) (Baum et al., 2009) to model the heavy storm triggered landslide event of 15 July 2006 in Jinbu-Myeon, Pyeongchang-gun, Korea. In this model, the physical parameters of soil, the Digital Elevation Model (DEM), and the real observed landslide scars as well as their rainstorm triggering are known. The influence of vegetation cover was considered in terms of tree root cohesion which was calculated by a trial-and-error method until the best match between the observed and predicted landslides was obtained. In the final step, when the tree root cohesion is estimated, the outputs of TRIGRS model is evaluated again by comparing with the observed landslide scars in locations, the slope angle of landslide initiation, and soil depth in unstable areas. Several grid cells were also examined to study the role of grid cell dimension on the precision of landslide prediction. These evaluations are the evidence to conclude if TRIGRS is suitable for applying in the study area.

2. Shear Strength of Forest Soil

The main effect of vegetation cover on the shear strength of forest soil is induced by the mechanical reinforcement of the soil caused by tree roots and the increased surcharge on the slope soil mantle. However, it is difficult to measure the strength of forest soil directly, and investigations at previously failed sites with accurate soil data are rare (Sidle & Ochiai, 2006). Many studies have reported a positive contribution of tree roots on the shear strength of soil; however, the question of how to best evaluate this influence remaining. Most studies have concluded that roots have only a negligible influence on the frictional component of soil strength due to their random orientation (Ziemer, 1981; O'Loughlin & Ziemer, 1982; Wu & Sidle, 1995; Sidle & Ochiai, 2006; Ali & Osman, 2008). Several studies have concluded that the root system contributes to shear strength by providing an additional cohesion component (ΔC) in the Mohr-Coulomb equation (Eq. (1)) (Gray & Megahan, 1981; O'Loughlin & Ziemer, 1982; Buchanan & Savigny, 1990; Abe & Ziemer, 1991; Schmidt et al., 2001), which is often defined as the "apparent cohesion" (Swanston, 1970; Wu et al., 1979):

$$s = (c' + \Delta C) + (\sigma - u)tan\phi' \quad (1)$$

where

c' is the effective cohesion of the soil (kN/m^2)

ϕ' is the effective internal angle of friction (degree)

ΔC is the apparent cohesion provided by roots (kN/m^2)

σ is the normal stress due to the weight of the soil (kN/m^2), and

u is the soil pore water pressure (kN/m^2)

The weight of trees might increase or decrease the overall slope stability depending on the type of soil and the slope parameters. The weight of trees influences slope stability in a positive way if due to the tree weight, the driving force does not exceed the resisting force and vice versa (Steinacher et al., 2009). More specifically, it is not possible to provide general conclusions about the positive or negative influence of tree surcharge on slope stability in cohesive soils (Gray, 1973). However, in non-cohesive soils, tree weight has a neutral to slightly positive effect for slope-parallel or curved sliding planes below the depth of the root system (Steinacher et al., 2009). Gray (1973) concluded that the tree surcharge

has a beneficial effect on stability, particularly when critical, saturated conditions develop in a slope. However, overall, consideration of tree surcharge as a negative impact may be neglected in most cases because it is not significant. This weight is often distributed uniformly throughout the entire area, and in most mature forest situations, the total weight of the soil and parent materials overlying a potential failure plane far exceeds the weight of the forest crop (Steinacher et al., 2009). Moreover, the positive influence of root reinforcement is more important than any adverse tree surcharge effects related to bank stability (O'Loughlin & Ziemer, 1982; Aberrnethy & BRutherfurd, 2000; Sidle & Ochiai, 2006).

In this study, as the soil cover layer is granular, field observation after the sliding event showed that the cover layer was almost fully saturated at failure. Therefore, it is possible to ignore the influence of tree surcharge for simplicity, and the mechanical effect of trees on soil shear strength is represented by the tree root cohesion (apparent cohesion).

3. Previous Methods for Determination of Root Cohesion

As discussed above, the contribution of tree roots to increasing soil shear strength is defined as the additional apparent cohesion that is added to the soil cohesion. According to O'Loughlin & Ziemer (1982), studies related to root strength and slope stability have been directed mainly in four distinct areas of endeavor: 1) direct field and laboratory measurement of the contribution to soil strength imparted by roots; 2) indirect computation of the contribution to soil strength made by roots using data of root strength, root density, root distribution, and root morphology; 3) development of theoretical slope stability analyses, in particular "back-analyses," using slope and soil physical data to estimate the contribution to soil strength made by roots; and 4) laboratory studies of the individual strengths of roots sampled from living trees and the rates at which root strength is lost after tree cutting.

Terwilliger & Waldron (1990), Abe & Ziemer (1991), Ali & Osman (2008), and Docker & Hubble (2008) applied the direct method in the laboratory using modified direct shear tests and laboratory measurements, Buroughs & Thomas (1977) and Gray & Megahan (1981) observed the concentration of intermingled lateral roots combined with the tensile strength of individual roots to estimate the total tensile strength per unit area of soil. Among indirect computations, Wu et al. (1979) developed a model that used only root critical tensile strength and the cross-sectional area of roots crossing the failure surface to estimate the shear strength of forested soil. All of these studies emphasized an increase in shear strength due to root reinforcement. The back-calculation approach was first applied by Gray (1973), who performed stability analyzes on failed slopes in Alaska. Using a simple form of the "method of slices", he assumed a safety factor of 1.0 at failure and derived values for c_a by back-calculation. It is widely accepted that the shear strength parameters obtained by back-analysis are more reliable than those obtained by laboratory or in-situ testing (Hussain et al., 2010; Zhang et al., 2012).

Estimates of vegetation root strength have been made from back-calculations of previously failed hillslopes where geotechnical and hydrological parameters were known or assumed (Swanston, 1970; Van Asch, 1984; Sidle & Ochiai, 2006). According to Lee & Hencher (2014), detailed studies of landslides including back-analysis is one of the most fruitful ways of advancing knowledge of landslide mechanisms to allow improved design and land management. In the back-analysis, the slope has already failed and the objective is to determine the value of some parameters in the analysis. In more detail, the factor of safety is set equal to one, and the values of an unknown are solved for (Skaugset, 1997). This method provides an estimate of the magnitude of reinforcement imparted to soils by tree roots (O'Loughlin, 1974) and may represent the best spatially distributed data available for root cohesion in the vicinity of a landslide, assuming that other input data are accurate (Sidle & Ochiai, 2006).

4. Application of Trigrs for Stability Assessment

This study applied TRIGRS (Baum et al., 2009) to predict the occurrence of landslides in the study area. The program has been used widely in many countries in recent years (Yuan et al., 2005; Salciarini et al., 2006; Baum et al., 2010; Liao et al., 2011; Kim et al., 2013; Park et al., 2013; Bordoni et al., 2014). TRIGRS is a coupled hydro-mechanical slope

stability assessment model that combines modules for infiltration and subsurface flow of storm water with those for runoff routing and slope stability. The infiltration process is modeled by a simplified analytical solution of Richards' equation (Eq. (2)), which requires a shallow, quasi-saturated soil cover at the beginning of the simulation. The solution of Iverson (2000) contains both steady and transient components. The steady infiltration rate, saturated hydraulic conductivity, and slope angle determine the steady (initial) flow direction. The transient component assumes one-dimensional, vertical, downward flow. This simplified Richards' equation in TRIGRS has the practical application that, according to Iverson (2000), the horizontal components can be neglected when the ratio of the soil depth to the square root of the contribution area $\left(\frac{H}{\sqrt{A}}\right)$ is much less than unity.

$$\frac{\partial\theta}{\partial t}=\frac{\partial}{\partial z}\left[K(\psi)\left(\frac{1}{\cos^2\delta}\frac{\partial\psi}{\partial z}-1\right)\right] \quad (2)$$

where

ψ is the ground-water pressure head (m);

θ is the volumetric water content;

t is the time (sec);

Z is the depth below the ground surface (m), and

δ is the slope angle (degree);

$K(\psi)$ is the hydraulic conductivity in Z direction (m/s).

In TRIGRS, the F_S value is calculated for transient pressure heads at multiple depths Z by using an infinite slope stability analysis (Taylor, 1948). In this analysis, the failure of an infinite slope is characterized by the ratio of the resisting basal Coulomb friction to the gravitationally induced downslope basal driving stress. This ratio is calculated at an arbitrary depth Z for each grid cell by the Eq. (3).

$$F_s(Z,t)=\frac{\tan\phi'}{\tan\delta}+\frac{c'-\Psi(Z,t)\gamma_w\tan\phi'}{\gamma_s Z\sin\delta\cos\delta} \quad (3)$$

where

Ψ is the ground-water pressure head as a function of depth Z and time t (m);

γ_w is the unit weight of water (kN/m^3), and

γ_s are the unit weights of soil (kN/m^3).

Failure is predicted when Fs < 1, and stability hold when $F_s \geq 1$. The state of limiting equilibrium exists when Fs = 1.

In order to take the contribution of tree roots into account in TRIGRS, as discussed in the previous sections, a component of tree cohesion (ΔC) is added, so Eq. (3) can be revised as following.

$$F_s(Z,t)=\frac{\tan\phi'}{\tan\delta}+\frac{(c'+\Delta C)-\Psi(Z,t)\gamma_w\tan\phi'}{\gamma_s Z\sin\delta\cos\delta} \quad (4)$$

The conceptual methodology of the TRIGRS model with the input parameters and output maps is illustrated in Fig. 1.

5. Landslide Evaluation

When comparing the actual with the predicted landslide grid-based maps, it is clear that four types of outcomes are possible: 1) actual sliding cells are predicted as unstable cells; 2) actual sliding cells are predicted as stable cells; 3) actual stable cells are predicted as unstable cells; and 4) actual stable cells are predicted as stable cells. Among the four types, type 1 and type 4 are classified as successfully predicted; type 2 and type 3 are classified as failed prediction. Based on the above classification, Montgomery & Dietrich (1994) introduced the Success Rate (SR) for landslide evaluation (Eq. (5)). This index takes type 1 into account but ignores

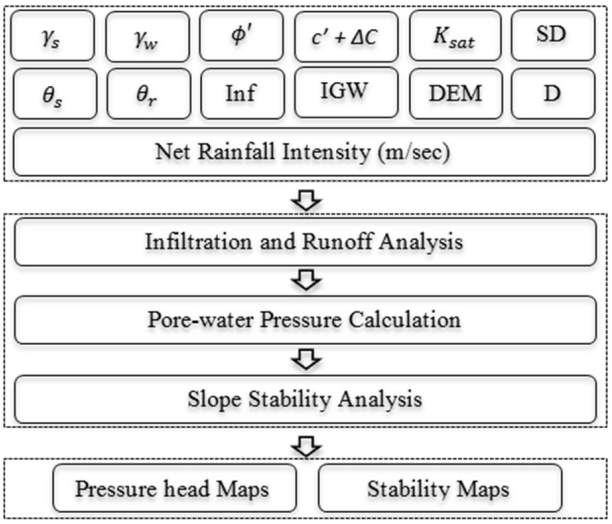

Fig. 1. Conceptual framework of the TRIGRS model: K_{sat} – the saturated hydraulic conductivity (m/sec), SD – the soil depth (m), θ_s – the saturated volumetric water content, θ_r – the residual volumetric water content, Inf – the Initial infiltration rate (m/sec), IGW – Initial groundwater level (m), D – Diffusivity (m^2/s)

the other three types.

$$SR = \frac{\text{number of successfully predicted landslides}}{\text{total number of actual landslides}} \quad (5)$$

From the equation, it is clear that by applying SR as a performance indicator, slope failure is overestimated (Huang & Kao, 2006; Bischetti & Chiaradia, 2010). As an extreme case, for example, if the whole area is classified as unstable, the resulting SR would be 100%. Based on the condition that the SR and the performance of stable cell prediction are weighted equally. Huang & Kao (2006) improved the SR equation by introducing the Modified Success Rate (MSR) (Eq. (6)) for evaluating the performance of landslide models.

$$MSR = 0.5 \times SR + 0.5 \times \frac{\text{successfully predicted stable cells}}{\text{total number of actual stable cells}} \quad (6)$$

The weighting factor of 0.5 was assigned according to results of the stochastic test and real-case application. The performance value derived by MSR ranges from 0.0～1.0 (Huang & Kao 2006). When MSR < 80%, landslide overprediction likely occurs. On the other hand, the MSR-derived performance values begin to decrease as stable coverage becomes higher than 90%, where landslide underprediction likely occurs. The best simulation derived by MSR would be around 80%～90% (Huang & Kao, 2006).

6. Methodology

The TRIGRS program is applied as the landslide prediction tool in this study. Based on all the known parameters which were defined by field tests, laboratory tests, or empirical estimations, such as the slope angle, the soil depth, soil engineering parameters, groundwater level, etc. The influence of tree roots on improving soil shear strength was estimated by the trial-and-error method. More specifically, various values of root cohesion were tested by the TRIGRS model. Each value provides a stability map (F_s map), and therefore, it is corresponding to a Modified Success Rate (MSR) value. The expected tree root value is the one that gives the most MSR value or the best stability map in compared to the observation.

It is obvious that when root cohesion is ignored or when small values of root cohesion are used, unstable areas (areas with $F_S < 1$) as well as overprediction trend (MSR is much smaller than 80%) is dominant. However, on the contrary, when higher values of root cohesion are applied, unstable areas are reduced, underprediction trend (MSR is larger than 90%) is likely to occur. Thus, there should be a suitable value of tree root cohesion that somehow provides a balance between the situation of underestimation and overestimation, and this value should correspond to the expected value of root cohesion.

The trial range of tree root cohesion begins from a value that ensures no unstable cells (cells with F_S <1) occurring in the initial condition. This is to satisfy the fact that the whole research site is stable before the rainstorm event. When the lower bound of tree root cohesion is defined, various values cohesion are tested by TRIGRS to find a relationship between MSR and the total soil cohesion. The one with the best MSR or the one that provides the most acceptable predicted stability map in comparison with the real landslide scars is the estimated tree root cohesion of the study area.

7. Study Area and Real Landslide Event

The research site is a small watershed located in Jinbu-Myeon, Pyeongchang-gun, Kangwon Prefecture, Republic of Korea. The center of the study area is located at 37°37′49″ N, 128°33′29″ E (Fig. 2). Rainfall-triggered debris flows, and shallow soil slides are the most abundant types of landslide occurrences in this area (Lee et al., 2012b). From 14 June to 29 July 2006, during the rainy season, very intense rainfall episodes caused many shallow landslides of the flow type in granular soils on the slopes. Because Jinbu was the most damaged area, it was a suitable site for evaluation of the frequency and the distribution of landslides (Lee et al., 2012c). Several studies about landslides in Jinbu-Myeon have been conducted to date (Lee et al., 2012b; Lee et al., 2012c; Kim et al., 2015a), but none of these took the physical influence of vegetation cover into account.

Due to a rainstorm even, some landslides were triggered between 13:00 and 14:00 (LT) on 15 July 2006. This exact time was determined by interviewing local people. The scars of these landslides were interpreted by digitizing the high-

resolution aerial photograph that was taken right after the landslide events (Fig. 7). The information on landslide scars extracted from aerial photos is generally based on the morphological, drainage and vegetational conditions of the slopes. However, in this study, only the last factor was considered as its clear vegetational contrast with surrounding and the lack of data related to the first two factors. These landslide scars were then adjusted and verified by using field survey descriptions.

7.1 Geomorphology

The surface of the study area is illustrated by a 1.0-m resolution elevation map which is created by the National Geographic Information Institute in the Republic of Korea (Fig. 3). This map was then used to interpolate the slope map (Fig. 4) and the flow directions map for the input files in TRIGRS model. As can be seen in Fig. 4, the area is composed of very steep slopes (average slope angle is almost

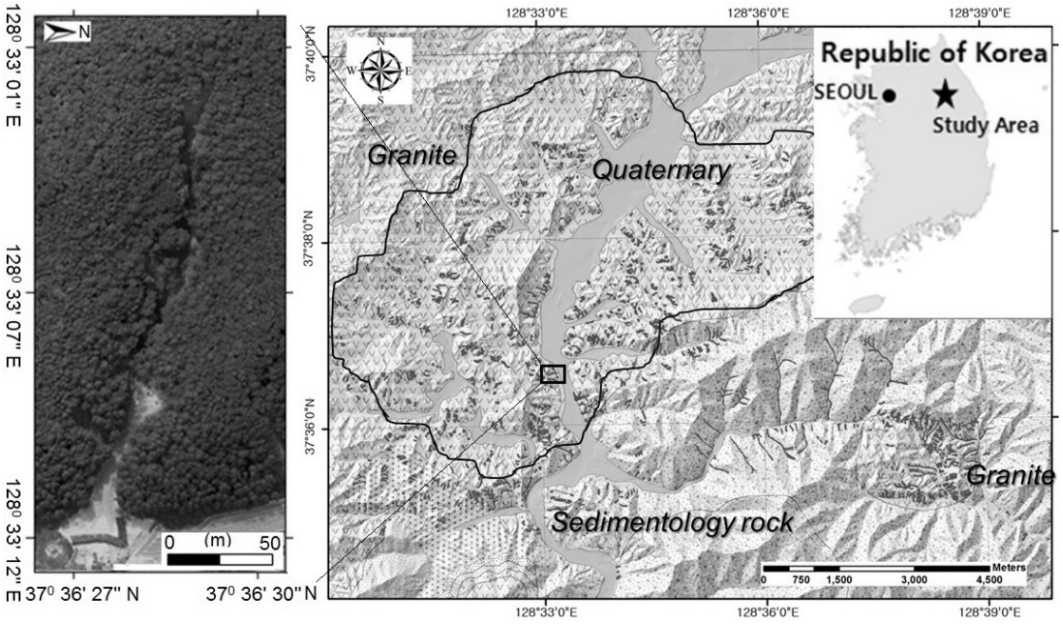

Fig. 2. Location of the study area (Kim et al., 2015b)

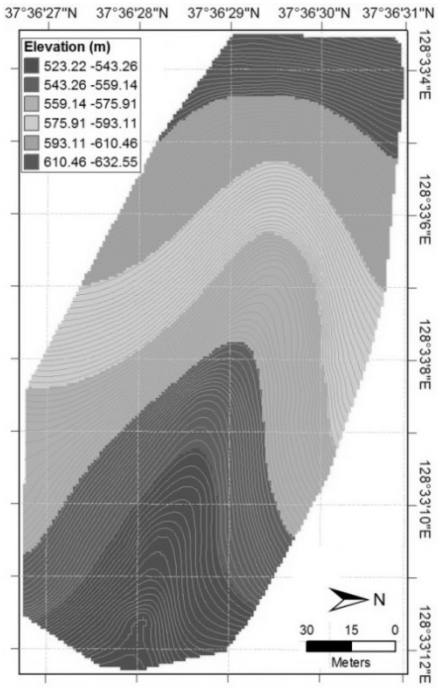

Fig. 3. Digital elevation model

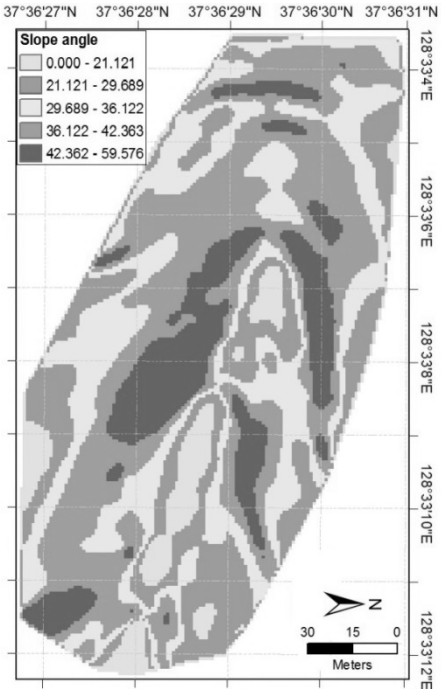

Fig. 4. Slope map

34 degrees; about 45% of the slope is steeper than the internal friction angle of 36.5°.

7.2 Geological Conditions and Soil Engineering Parameters

The Imgye Granite, which is an extensive intrusion of granitoids that occurred during the Daebo Orogeny, is distributed over most of Jinbu-Myeon (about 77%), as shown in Fig. 2. The soil material of the study site is mostly granite residuum (Lee et al., 2012c), and well-drained soils cover about 84% of the whole area. Therefore, only one property zone is considered in this study.

For shear strength parameters of the soil cover layer, the triaxial test was conducted because it represents the processes and characteristics of the superficial soil layer better than the direct shear test (Frank et al., 2009; Kim et al., 2015a). Soil samples were collected from the field and then tested using the triaxial compression test. Shallow landslides are triggered by elevated pore pressure that decreases the effective normal stress rather than by increased shear stress (Anderson & Riemer, 1995). Unlike typical triaxial shear testing that is accomplished by increasing the shear stress, the Consolidated Drained (CD) test approximates the conditions during rainfall-induced failure by maintaining constant shear stress while reducing effective stress (Kim et al., 2015a). The results of the CD test are shown in Table 1.

At the same time as soil shear strength parameters were tested, the hydraulic conductivity, the dry and saturated soil densities, and the volumetric water content were also defined. Two input parameters for the unsaturated flow, the saturated volumetric water content (θ_s) and the residual volumetric water content θ_r, were determined by using the Soil Water Characteristic Curve (SWCC) test. The SWCC (Fig. 5) was drawn by fitting the van Genuchten formula, and the saturated and residual volumetric water contents determined from it were 49.6% and 15.0%, respectively (Table 1).

Other input parameters for TRIGRS including the diffusivity (D_0) and the steady infiltration rate (I_Z) were estimated from empirical references because their values have a wide range and depend on many factors (Hanks & Bowers, 1963; Iverson, 2000). Iverson (2000) identified D_0 as the maximum characteristic diffusivity given by the ratio of saturated conductivity (K_{sat}) to the minimum value of the change in volumetric water content per unit change in a pressure head (C_0). The larger the value of diffusivity, the faster the downward propagation of groundwater. As it is difficult to test for D_0, several studies have defined the range of D_0 as being from 5～500 times that of the hydraulic conductivity (Yuan et al., 2005; Liu & Wu, 2008; Baum et al., 2010; Kim et al., 2010a; Liao et al., 2011; Park et al., 2013). In this study, based on the hydraulic properties of the soil, D_0 was assumed to be 100 times the value of K_{sat}. The value of I_z can be approximated by defining the average precipitation rate needed to maintain the initial conditions in the days and months preceding an event (Baum et al., 2010). However, for simplification, I_z was assumed to be 100 times less than K_{sat}, as suggested by Park et al. (2013) due to the conditions during summer in Korea.

7.3 Groundwater Table and Rainfall Data

There were no groundwater table data before the landslide incident. However, based on the natural conditions of the hillslopes in Korea, groundwater commonly lies in the very deep soil around the mountain tops of South Korea (Kim et al., 2013). Therefore, most studies have accepted that the groundwater table coincides with the depth of the top soil

Table 1. Soil properties tested by triaxial test

Soil parameter	Unit	Value
Saturated soil density	kN/cm^3	17.4
Unsaturated soil density	kN/cm^3	14.9
Water density	kN/cm^3	10
Cohesion c	kPa	1.6
Internal friction angle ϕ	(°)	36.5
Hydraulic conductivity K_{sat}	m/s	1.389 E-05
Diffusivity D_0	m^2s^{-1}	100 × K_{sat}
Steady infiltration rate I_z	m/s	0.01 × K_{sat}

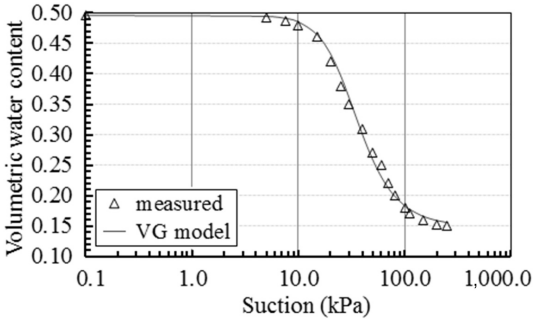

Fig. 5. Soil water characteristic curve in the study area

layers at initial condition (Kim et al., 2010a; Kim et al., 2013; Park et al., 2013). Thus, in this study, the event occurred during the summer, and there was no heavy antecedent rainfall before the event, the groundwater table was assumed to be at the bottom of the weathered soil layer (Fig. 8).

Rainfall occurs primarily during the summer season, from June to September, as part of the East Asian monsoon (Kim et al., 2015a). Jinbu, in the Pyeongchan District, is within the rainiest area in Korea. Its total precipitation is more 750 mm than the annual ones of 340 mm during the rainy season. Of particular significance, heavy rainfall totaling 429 mm fell in the study area over a period of more than 29 h on 15～16 July 2006. Kim et al. (2015b) measured the total rainfall rate at 450 mm day^{-1} and the maximum rainfall intensity of the triggering event at about 90 mm h^{-1}. This critical condition led to many landslides, the collapse of embankments, and the flooding of farmland due to water level increases at the confluence of rivers (Lee et al., 2012a; Lee et al., 2012b).

It has frequently been observed that hillslope failures are often related to short (<1 h) and intense rainfall rather than to daily-average precipitation (Kim et al., 2015b). Therefore, in this study, a time series of rainfall intensity per 30 min was used as the input in the TRIGRS model. The data was measured by Jinbu-Myeon station corresponding to the landslide event that started at 00:00 on 15 July 2006 and ended at 16:00 on the same day. Fig. 6 shows the measured 30-min rainfall intensity in the study area before, during, and after the sliding event occurred.

7.4 Forest Properties

Pyeongchang had 37.1% of coniferous forest, 39.7% of deciduous forest, and 23.2% of mixed forest cover. The crown coverage value was mostly medium or dense. The study area was under Korean pine (Pinus koraiensis) and Japanese larch (Larix kaempferi) (Kim et al., 2015b) (Fig. 7), which are two common plantation species in Korea (Kim et al., 2011). The estimated root reinforcements from the model of Wu et al. (1979) were, on average, 4.04 kPa for Japanese larch and 12.26 kPa for Korean pine (Kim et al., 2011). However, these values may vary depending on species, root density, soil properties, and assessment methods.

7.5 Soil Depth or Soil Thickness

Soil thickness is of particular importance, as are the mechanical and hydrological properties related to hydraulic conductivity, transmissivity, and angle of internal friction (Kim et al., 2015a). However, mapping the thickness of the topsoil layer is complex, costly, and time-consuming, especially for a large area with complicated topography. Therefore, soil thickness information has rarely been obtained from landslide-prone areas, and uniform soil thickness has often been assumed (Ho et al., 2012; Park et al., 2013). Several researchers have created a soil thickness map using the relationship between soil thickness and topographical conditions (Salciarini et al., 2006; Segoni et al., 2012). Lee & Ho (2009) adopted the wetness index to determine the spatial distribution of soil thickness for a slope stability analysis. In this study, the dynamic cone penetrometer (25 mm diameter

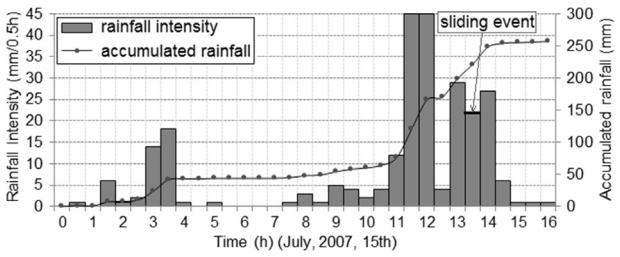

Fig. 6. Thirty minute rainfall intensity data

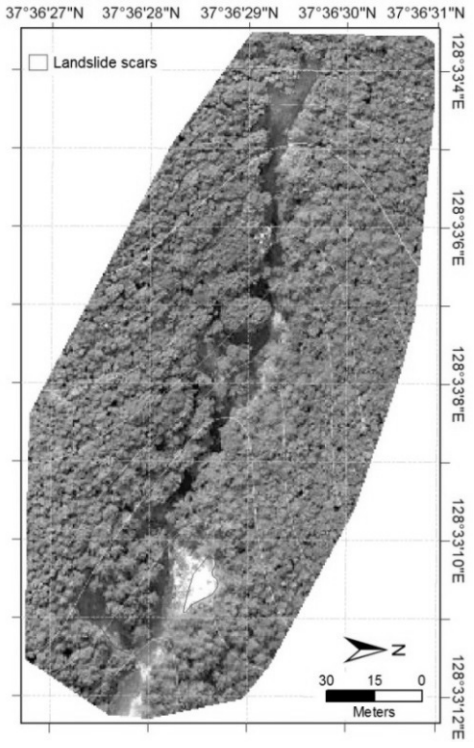

Fig. 7. Vegetation coverage and landslide scar map

with 60° tip angle), also known as the knocking pole test was used to measure the soil thickness data in the study area, where landslides have increased recently. More detail about the procedure to build the soil thickness map is described in the study of Kim et al. (2015b). The map shows the thickness of the weathered soil layer is presented in Fig. 8 in meter.

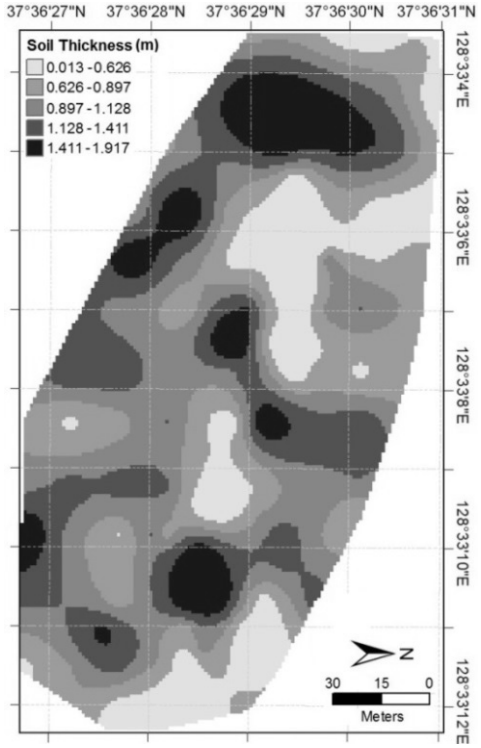

Fig. 8. Map of Soil thickness

8. Trial-And-Error Method for the Determination of Tree Root Cohesion

Fig. 9 shows the FS map at the initial condition when root cohesion is not taken into account. As can be seen, a large proportion of the study area is unconditionally unstable or with the present input data; these areas are unstable under all kind of rainfall scenarios. This is not reasonable in reality as the slopes remain stable. By applying the trial-and-error method, and increasing the value of total cohesion until there was no unstable cell in the F_S map at initial condition (Fig. 10), the lower bound of root cohesion was found to be equal to 3 kPa.

After the lower bound of tree root cohesion was defined, the trial-and-error procedure was continued; however, the MSR value of each F_S map corresponding to each trial of root cohesion also was started to calculate. As explained in

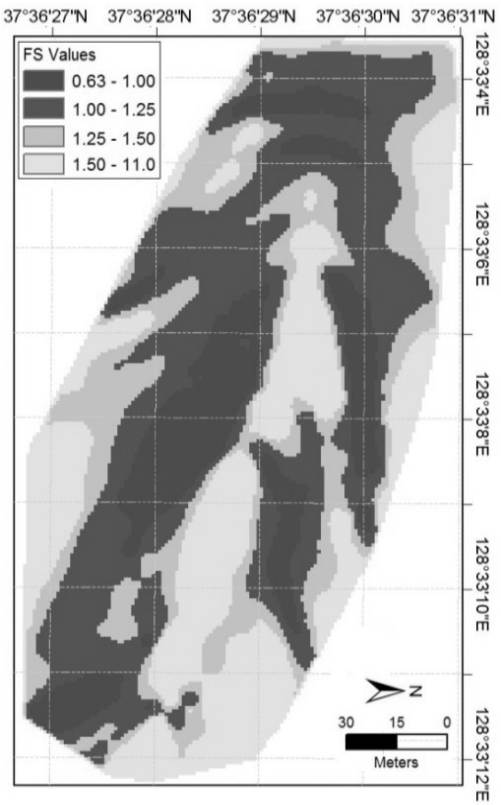

Fig. 9. FS map at initial condition when tree root cohesion is ignored

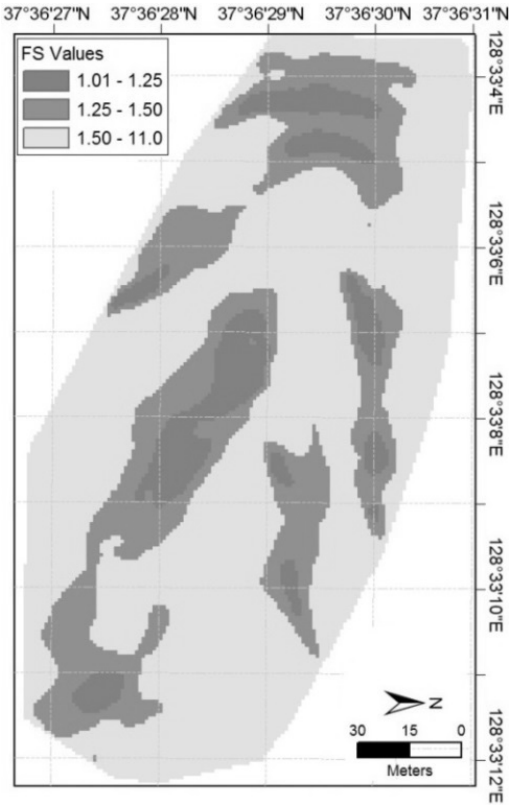

Fig. 10. FS map at initial condition when tree root cohesion is considered (C_r = 3.0 kPa)

the methodology section, the procedure is stopped when there is a reducing trend in the value of MSR. This reducing trend indicates that the value of root cohesion begins to become larger than expected, creating an underprediction problem. Fig. 11 shows the relationship between MSR at the observed sliding time and different total cohesion (soil cohesion + root cohesion). As can be seen, the relationship has a smooth "dome" shape with the highest MRS value equal to 77.6%, which corresponds to the total cohesion of 5.4 kPa and the root cohesion of 3.8 kPa. This root cohesion value is not much different from the values estimated for the same types of trees (4.04 kPa for Japanese larch and 12.26 kPa for Korean pine) by Kim et al. (2011). Kim et al. (2010b) also concluded that roots increased soil shear strengths by as much as 3.9～28.2 kPa for larch and 13.5～35.4 kPa for Korean pine, implying that roots have substantial effects on slope stability. However, additional studies, both theoretical and experimental, need to be conducted to support this conclusion, especially for different local areas.

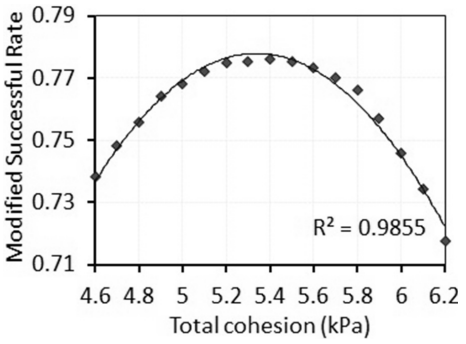

Fig. 11. Relationship between MSR at the observed sliding time and total cohesion

9. Results at the Critical Step Using the Selected Tree Root Cohesion

9.1 Time Variation of F_S

When the root cohesion is assigned, a series of F_S maps with time is created to see how the F_S values change within the duration of the rainfall. Figs. 12 to 15 show the distribution of F_S at four important main moments: 1) at the first peak of rainfall intensity (at 03:30 AM); 2) before beginning of the second peak (at 11:00 AM); 3) at the maximum rainfall intensity (at 12:00); and 4) at the time when most of the landslides occurred (13:30 PM). As can be seen, the unstable area becomes wider with time; in the same way, the MSR

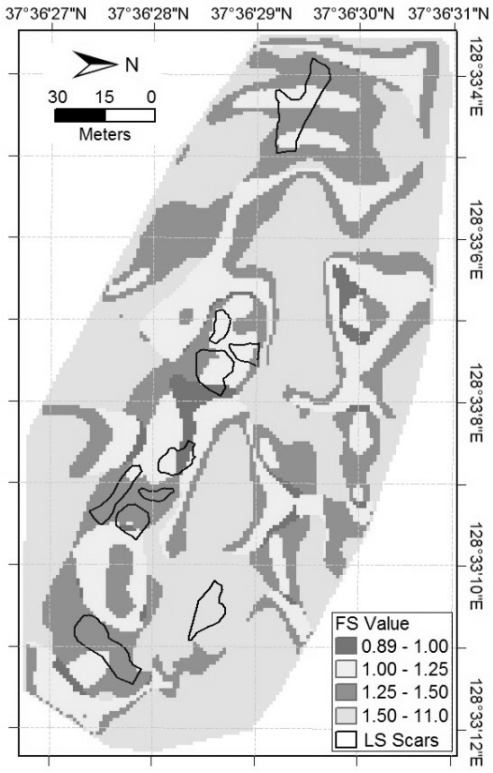

Fig. 12. FS map at 03h30', July 2007, 15th (SR = 5.14%; MSR = 51.34)

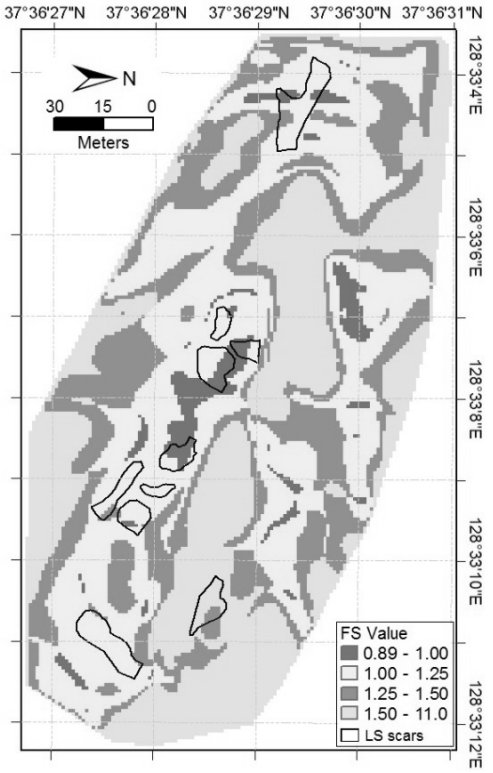

Fig. 13. FS map at 10h30', July 2007, 15th (SR = 15.87%; MSR = 56.21%)

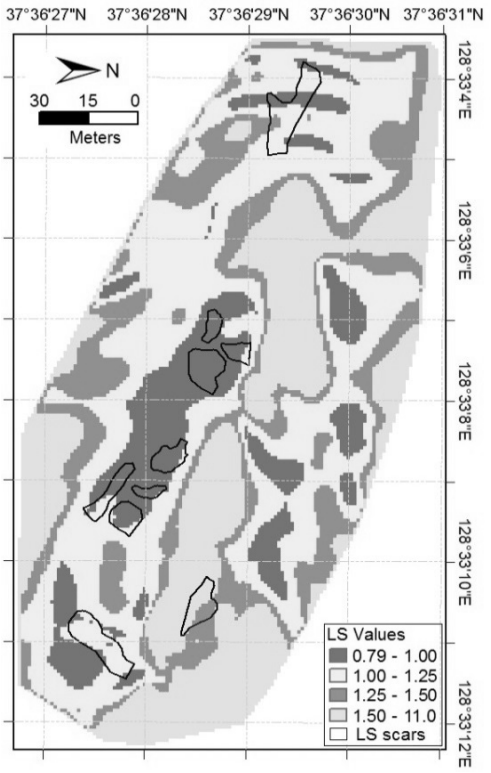

Fig. 14. FS map at 12h00, July 2007, 15th
(SR = 48.49%; MSR = 67.9%)

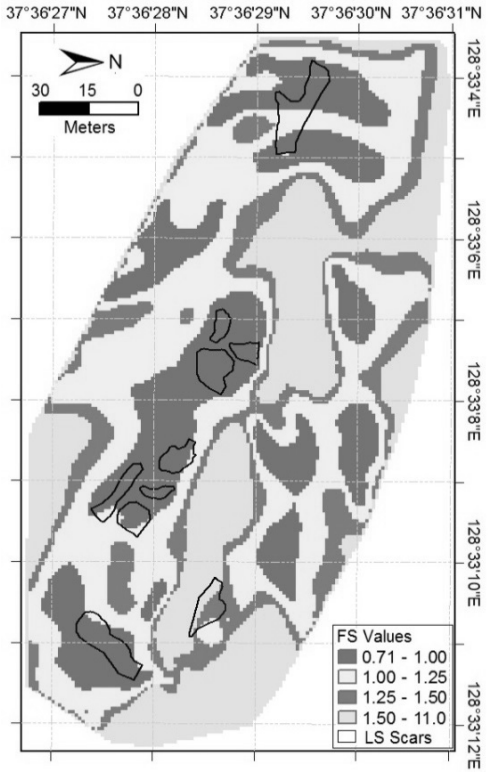

Fig. 15. FS map at 13h30, July 2007, 15th
(SR = 76.65%; MSR = 77.62%)

values also increase until the time of failure. As the same as the observation, most of the landslides do not occur at maximum rainfall intensity (Fig. 14), but rather 90 minutes later (Fig. 15). At the time of failure, 76.65% (based on Eq. 5) of the actual unstable cells are predicted, whereas 78.6% (based on Eq. (6)) of the actual stable cells are well predicted.

9.2 Consideration of Different Cell Size

Process-based models have been based on the infinite slope form of the Mohr-Coulomb failure law, in which landslide dimensions are ignored and these models nonetheless treat each grid cell independently (Casadei et al., 2003). Thus, their performance depends significantly on the quality of the topographic data as well as the relative sizes of the landslides compared to the grid cell dimensions (Gritzner et al., 2001). However, most of the previous studies did not examine in detail the optimal grid cell size for assessing landslide susceptibility (Uchida et al., 2011). Therefore, when the tree root cohesion is defined, a step to evaluate the influence of the raster cell size on the predicted landslide map is necessary. This study examined five cases: 1.0 m, 2.0 m, 3.0 m, 4.0 m, and 5.0 m. A TRIGRS model was built

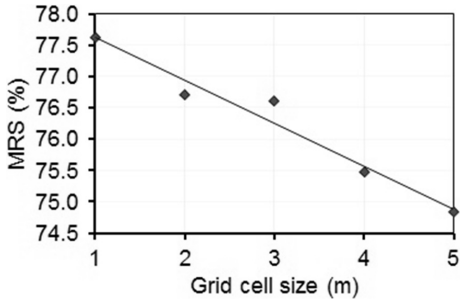

Fig. 16. Value of MRS at different grid cell sizes

for each grid size case, and their MSR values were also calculated.

Fig. 16 shows the relationship between MSR and the different cell sizes. As can be seen, among five study cases, the 1.0 m × 1.0 m size provided the best result; smaller cell sizes give better prediction results. This conclusion is coinciding with the study of Uchida et al. (2011) and Kim et al. (2015b). However, it might change when different sites are considered, higher resolution does not necessarily means better model performances (Penna et al., 2014; Tarolli & Tarboton, 2006) because the relative sizes of the landslides compared to the grid cell dimensions is the deciding factor.

9.3 Consideration of Study Area Slope Angles

For slope angle assessment, the slope angle values of the real landslide scars (Fig. 17) and the predicted landslides (Fig. 18) were extracted by combining the predicted F_S map at the critical time (Fig. 15) and the slope map (Fig. 4). As can be seen, although some scatters occur in the values between the slopes of the real and predicted landslides, in both cases, the largest occurrence of landslides falls within the interval of slope angles ranging from 36.5° to 46.5° or in the narrower range from 39° to 44°. In general, landslides tend to occur on steeper slopes in the predicted model compared with the observed scars.

9.4 Consideration of Soil Thickness of the Study Area

When it comes to the soil thickness of the unstable area, the histogram of the predicted sliding depth is left-skewed (Fig. 19) showing the range of soil depth with the highest landslide frequency from 1.02 m to 1.32 m, but the histogram of observed sliding depth (Fig. 20) does not show such a clear pattern. Observed landslides occur more often in the depth range of 1.02 m to 1.32 m, but a large frequency of landslides also occurs in the 1.72 m to 1.82 m interval. Additionally, the soil depth of the observed landslides is slightly larger than that of the predicted landslides (average value of 1.347 m compared to 1.228 m).

10. Conclusion

Like other numerical and analytical models of groundwater flow and slope stability, TRIGRS is subjected to limitations imposed by simplifying assumptions, approximations, and other shortcomings in the underlying theories (Baum et al., 2009). Beside some limitations, those can be relieved by the site conditions themselves, such as the soil is assumed to be homogeneous and isotropic, the flow is presumed to be one-dimensional vertical infiltration. Other things can be done to improve the performance of the model are to improve the quality of the input data such as the groundwater conditions, the DEM, the spatial distribution of soil depth, and the soil

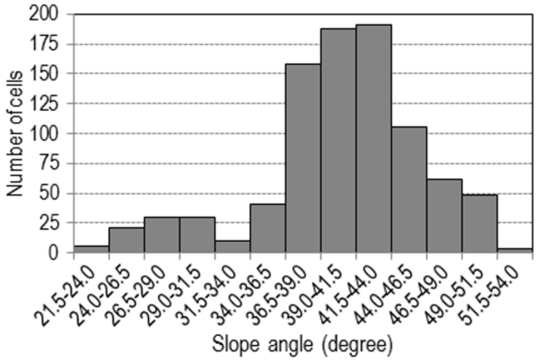

Fig. 17. Slope angle of real landslide scars
(Min = 22.62; Mean = 40.47; Max = 52.06)

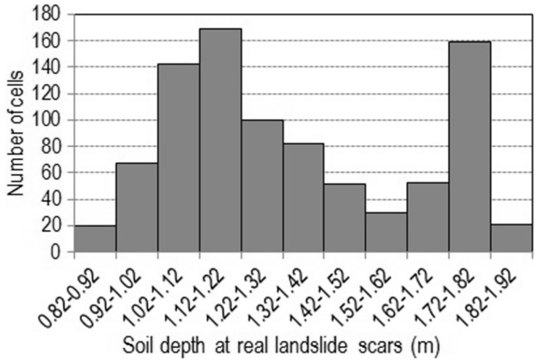

Fig. 19. Soil thickness of real landslide scars
(Min = 0.821; Mean = 1.347; Max = 1.903)

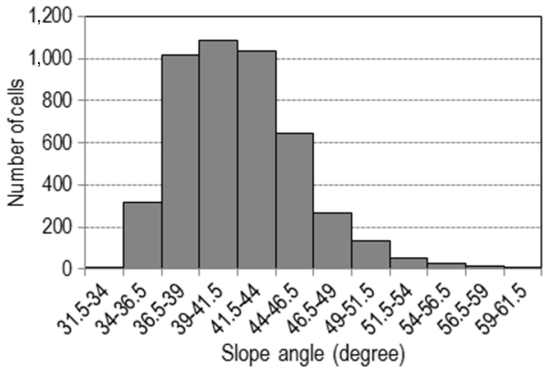

Fig. 18. Slope angle of predicted landslide scars
(Min = 33.74; Mean = 41.6; Max = 59.576)

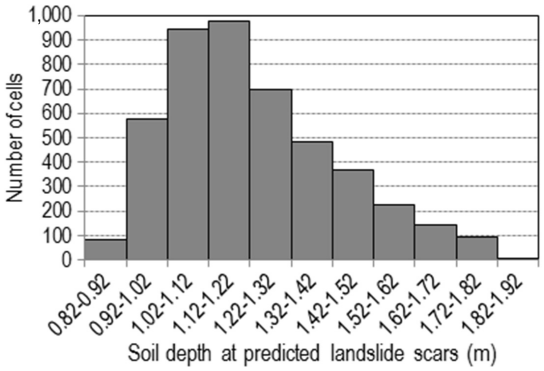

Fig. 20. Soil thickness of predicted landslide
(Min = 0.858; Mean = 1.228; Max = 1.833)

engineering parameters. More details about the limitations of the TRIGRS model are well concluded in the study of Baum et al. (2009). Within this study, the following conclusions can be drawn:

Root cohesion plays a significant role in stabilizing natural hillslope. Without considering its influence, a large proportion of the study area examined here would be unconditionally unstable even at the initial condition. Landslide models provide more reasonable results in both space and time when vegetation cover is considered.

This study used triaxial tests to determine soil shear strength and historical landslide scars to perform back-analysis of tree root cohesion. The impact of vegetation cover in the study area can be compared to an increase in soil cohesion of 3.8 kPa. However, more studies, both theoretical and experimental, need to be conducted to support this conclusion. Nevertheless, this study provides a good beginning on which engineers can base on for urban planning and designing.

When using a physical raster-based landslide model, the predicted landslides depend strongly on the quality of the topographic data and the relative size of the landslides compared to grid-cell dimensions. Therefore, additional studies should be conducted to determine the influence of cell size to predicted results. In this study, smaller cell sizes provided better results.

This study revealed a good match between the slope angles of real landslide scars and those of the predicted landslides, with the largest occurrence of landslides for both cases falling within the interval of slope angles from 36.5° to 46.5°. Thus, slope is a very good indicator for landslide prediction in the study area.

An analysis of the soil depth for the observed and the predicted landslides did not show good agreement, even though both of these showed that the highest frequency of landslide occurrence was within the soil thickness range of 1.02 m to 1.32 m. The average soil depth of the observed landslides was slightly larger than that of the predicted landslides (1.347 m compared to 1.228 m).

In short, further studies to quantify the impacts of trees on shallow landslides under various conditions of rainfall and topography are regarded as important for improving the model. Directly considering the influence of root cohesion is difficult because it depends on many factors, including depth of root, dimension of root, type of root, depth of root infiltration, and spatial variability of root cohesion. Thus, back-calculation based on historical landslides or old landslide scars is a good approach.

Acknowledgement

This subject is supported by Korea Ministry of Environment (MOE) as “GAIA Program-2014000 540005”.

References

1. Abe, K. and Ziemer, R. R. (1991), Effect of tree roots on shallow-seated landslides. Proceeding of the IUFRO technical session on geomorphic hazards in managed forests; Montreal, Canada, Department of Agriculture, pp. 11~20.
2. Aberrnethy, B. and BRutherfurd, I. D. (2000), The effect of riparian tree roots on the mass-stability of riverbanks, Earth Surface Processes and Landforms, Vol. 25, pp. 921~937.
3. Ali, F. H. and Osman, N. (2008), Shear strength of a soil containing vegetation roots, Japanese Geotechnical Society, Vol. 48, No. 4, pp. 587~596.
4. Anderson, S. and Riemer, M. (1995), Collapse of saturated soil due to reduction in confinement, Journal of Geotechnical Engineering, Vol. 121, No. 2, pp. 216~220.
5. Baum, R. L., Godt, J. W. and Savage, W. Z. (2010), Estimating the timing and location of shallow rainfall-induced landslides using a model for transient, unsaturated infiltration, Journal of Geophysical Research, Vol. 115, No. 3, pp. 1~26.
6. Baum, R. L., Savage, W. Z. and Godt, J. W. (2009), TRIGRS —A fortran program for transient rainfall infiltration and gridbased regional slope-stability analysis, Version 2.0. Colorado, U.S. Geological Survey, pp. 1~26.
7. Bischetti, G. B. and Chiaradia, E. A. (2010), Calibration of distributed shallow landslide models in forested landscapes, Journal of Agricultural Engineering, Vol. 41, No. 3, pp. 23~35.
8. Bordoni, M., Meisina, C., Valentino, R., Bittelli, M. and Chersich, S. (2014), From slope-to regional-scale shallow landslides susceptibility assessment using TRIGRS, Nat. Hazards Earth Syst. Sci, Vol. 2, No. 12, pp. 7409~7464.
9. Buchanan, P. and Savigny K. W. (1990), Factors controlling debris avalanche initiation, Can. Geotech. Journal, Vol. 27, No. 5, pp. 659~675.
10. Buroughs, E. R. and Thomas, B. R. (1977), Declining root strength in douglas-fit after felling as a factor in slope stability, USDA Forest Service Research Paper, Vol. 190, pp. 1~27.
11. Casadei, M., Dietrich, W. E. and Miller, N. (2003), Controls on shallow landslide size, in D. Rickenmann and C.L. Chen (eds), Debris-Flow Hazards Mitigation: Mechanics, Prediction, and Assessment, Davos, Switzerland, (Rotterdam: Millpress), pp. 91~101.
12. Docker, B. B. and Hubble, T. C. T. (2008), Quantifying rootreinforcement of river bank soils by four Australian tree species, Geomorphology, Vol. 100, No. 3~4, pp. 401~418.

13. Frank, G., Frei, M. and Boll, A. (2009), Effects of vegetation on the angle of internal friction of a moraine, For. Snow Landsc. Res, Vol. 82, No. 1, pp. 61~77.
14. Gray, D. H. (1973), Effects of forest clear-cutting on the stability of natural slopes: results of field studies, National Science Foundation. University of Michigan, Washington, pp. 45~66.
15. Gray, D. H. and Megahan, W. F. (1981), Forest vegetation removal and slope stability in the idaho batholith, For. Serv., U.S. Dep. of Agric, pp. 1~23.
16. Gritzner, M. L., Marcus, W. A., Aspinall, R. and Custer, S. G. (2001), Assessing landslide potential using GIS, soil wetness modeling and topographic attributes, Payette River, Idaho, Geomorphology, Vol. 37, No. 1~2, pp. 149~165.
17. Hanks, R. J. and Bowers S. A. (1963), Influence of variations in the diffusivity water content relation on infiltration, Soil Science Society of America Journal, Vol. 27, No. 3, pp. 263~265.
18. Ho, J. Y., Lee, K. T., Chang, T. C., Wang, Z. Y. and Liao, Y. H. (2012), Influences of spatial distribution of soil thickness on shallow landslide prediction, Engineering Geology, Vol. 124, No. 4, pp. 38~46.
19. Huang, J. C. and Kao, S. J. (2006), Optimal estimator for assessing landslide model performance, Hydrol. Earth Syst. Sci, Vol. 10, No. 6, pp. 957~965.
20. Hussain, M., Stark, T. D. and Akhtar, K. (2010), Back-analysis procedure for landslides, International Conference on Geotechnical Engineering. S. Kibria, H. M. Qureshi and A. M. Rana. Lahore, Pakistan, Pakistan Geot. Eng. Society, pp. 159~166.
21. Iverson, R. M. (2000), Landslide triggering by rain infiltration, Water Resources Research, Vol. 36, No. 7, pp. 1897~1910.
22. Jakob, M. (2000), The impacts of logging on landslide activity at clayoquot sound, british columbia, Cantena, Vol. 38, No. 4, pp. 279~300.
23. Kim, D., Lee, S. H. and Im, S. (2011), Analysis of the effect of tree roots on soil reinforcement considering its spatial distribution, J. Korean Env. Res. Tech, Vol. 14, No. 4, pp. 41~54.
24. Kim, D., Im, S., Lee, C. and Woo, C. (2013), Modeling the contribution of trees to shallow landslide development in a steep, forested watershed, Ecological Engineering, Vol. 61(C), pp. 658~668.
25. Kim, D., Im, S. and Lee, S. H. (2010a), Predicting the rainfalltriggered landslides in a forested mountain region using TRIGRS model, Journal of Mountain Science, Vol. 7, No. 1, pp. 83~91.
26. Kim, D., Lee, S. H., Combalicer, E. A., Hong, Y. and IM, S. (2010b), Estimating soil reinforcement by tree roots using the perpendicular root reinforcement model, International Journal of Erosion Control Engineering, Vol. 3, No. 1, pp. 80~84.
27. Kim, M. S., Onda, Y. and Kim, J. K. (2015a), Improvement of shallow landslide prediction accuracy using soil parameterisation for a granite area in South Korea, Nat. Hazards Earth Syst. Sci, Vol.3, No. 1, pp. 227~267.
28. Kim, M. S., Onda, Y., Kim, J. K. and Kim, S. W. (2015b), Effect of topography and soil parameterisation representing soil thicknesses on shallow landslide modelling, Quaternary International, Vol. 384, pp. 91~106.
29. Lee, K. T. and Ho, J. Y. (2009), Prediction of landslide occurrence based on slope-instability analysis and hydrological model simulation, Journal of Hydrology, Vol. 375, No. 3, pp. 489~497.
30. Lee, M. J., Choi, J., Park, I. and Lee, S. (2012a), Ensemblebased landslide susceptibility maps in Jinbu area, Korea, Environb Earth Sci, Vol. 67, No. 1, pp. 23~37.
31. Lee, S., Hwang, J. and Park, I. (2012b), Application of datadriven evidential belief functions to landslide susceptibility mapping in Jinbu, Korea, Catena, Vol. 100, pp. 15~30.
32. Lee, S., Song, K. Y., Oh, H. J. and Choi, J. (2012c), Detection of landslides using web-based aerial photographs and landslide susceptibility mapping using geospatial analysis, International Journal of Remote Sensing, Vol. 33, No. 16, pp. 4937~4966.
33. Lee, S. C. and Hencher, S. R. (2014), Recent extreme rainfallinduced landslides and government countermeasures in korea. Landslide Science for a Safer Geoenvironment. K. Sassa, P. Canuti and Y. Yin (eds), New York, Springer, Vol. 1, pp. 357~361.
34. Liao, Z., Hong, Y., Kirschbaum, D., Adler, R. F., Gourley, J. J. and Wooten, R. (2011), Evaluation of TRIGRS (transient rainfall infiltration and grid-based regional slope-stability analysis)'s predictive skill for hurricane-triggered landslides: a case study in macon county, north carolina, Nat. Hazards, Vol. 58, No. 1, pp. 325~339.
35. Liu, C. N. and Wu, C. C. (2008), Mapping susceptibility of rainfall-triggered shallow landslides using a probabilistic approach, Environ Geol, Vol. 55, No. 4, pp. 907~915.
36. Montgomery, D. R. and Dietrich, W. E. (1994), A physically based model for the topographic control on shallow landsliding, Water Resour. Res., Vol. 30, No. 4, pp. 1153~1171.
37. O'Loughlin, C. (1974), The effect of timber removal on the stability of forest soils, Journal of hydrology (N.Z.), Vol. 13, No. 2, pp. 121~134.
38. O'Loughlin, C. and Ziemer, R. R. (1982), The importance of root strength and deterioration rates upon edaphic stability in steepland forests. Proceedings of I.U.F.R.O. Workshop P.1.07-00 Ecology of Subalpine Ecosystems as a Key to Management, Oregon State University, Miscellaneous Publ, pp. 70~78.
39. Park, D. W., Nikhil, N. V. and Lee, S. R. (2013), Landslide and debris flow susceptibility zonation using TRIGRS for the 2011 Seoul landslide event, Nat. Hazards Earth Syst. Sci, Vol. 1, No. 3, pp. 2547~2587.
40. Penna, D., Borga, M., Aronica, G. T., Brigandi, G. and Tarolli, P. (2014), The influence of grid resolution on the prediction of natural and road-related shallow landslides, Hydrol. Earth Syst. Sci, Vol. 18, No. 6, pp. 2127~2139.
41. Salciarini, D., Godt, J. W., Savage, W. Z., Conversini, P., Baum, R. L. and Michael, J. A. (2006), Modeling regional initiation of rainfall-induced shallow landslides in the eastern Umbria Region of central Italy, Landslides, Vol. 3, No. 3, pp. 181~194.
42. Schmidt, K. M., Roering, J. J., Stock, J. D., Dietrich, W. E., Montgomery, D. R. and Schaub, T. (2001), The variability of root cohesion as an influence on shallow landslide susceptiblity in the oregon coast range, Can. Geotech, Vol. 38, No. 5, pp. 995~1024.
43. Schwarz, M., Giadrossich, F. and Cohen, D. (2013), Modeling root reinforcement using root-failure weibull survival function, Hydrol. Earth Syst. Sci, Vol. 17, No. 11, pp. 4367~4377.

44. Segoni, S, Rossi, G, Catani, F. (2012), Improving basin scale shallow landslide modelling using reliable soil thickness maps, Nat. Hazards, Vol. 61, No. 1, pp. 85~101.
45. Sidle, R. C. and Ochiai, H. (2006), Landslides processes, prediction, and land use. Washington, DC, American Geophysical Union, pp. 1~312.
46. Skaugset, A. E. (1997), Modelling root reinforcement in shallow forest soils. Oregon State University, Oregon State University libraries. PhD Thesis, pp. 1~300.
47. Steinacher, R., Medicus, G., Fellin, W. and Zangerl, C. (2009), The influence of deforestation on slope (in-) stability, Austrian journal of earth sciences, Vol. 102, No. 2, pp. 90~99.
48. Swanston, D. N. (1970), Mechanics of debris avalanching in shallow till soils of southeast alaska, USDA Forest Service Research Paper PNW, Vol. 103, pp. 121~134.
49. Swanston, D. N. and Marion D. A. (1991), Landslide response to timber harvest in southeast alaska, Proceeding of the Fifth Interagency Sedimentation Conference, Las Vegas, Nevada, Federal Energy Regulatory Commission, pp. 10~49.
50. Tarolli, P. and Tarboton, D. G. (2006), A new method for determining of most likely landslide initiation points and the evaluation of digital terrain model scale in terrain stability mapping, Hydrol. Earth Syst. Sci, Vol. 10, No. 5, pp. 663~677.
51. Taylor, D. W. (1948), Fundamentals of soil mechanics. New York, John Wiley & Sons, Inc, pp. 1~712.
52. Terwilliger, V. J. and Waldron, L. J. (1990), Assessing the contribution of roots to the strength of undisturbed, slip prone soils, Catena, Vol. 17, pp. 151~162.
53. Uchida, T., Tamur, K. and Akiyama, K. (2011), The role of grid cell size, flow routing algolithm and spatial variability of soil depth on shallow landslide prediction, Italian Journal of Engineering Geology and Environment – Book, Vol. 11, pp. 149~157.
54. Van Asch, T. W. J. (1984), Landslides: The deduction of strength parameters of materials from equilibrium analysis, Catena, Vol. 11, pp. 39~49.
55. Wu, T. H., McKinnell, W. P. and Swanston, D. N. (1979), Strength of tree roots on prince of wales island, alaska, Can. Geotech, Vol. 16, No. 1, pp. 19~33.
56. Wu, W. and Sidle, R. C. (1995), A distributed slope stability model for steep forested basins, Water Resour. Res, Vol. 31, No. 8, pp. 2097~2110.
57. Yuan, C. C., Chien, C. T., Chieh, Y. F. and Chi, L. S. (2005), Analysis of time-varying rainfall infiltration induced landslide, Environ Geol, Vol. 48, No. 4, pp. 466~479.
58. Zhang, K., Cao, P. and Bao, R. (2012), Rigorous back analysis of shear strength parameters of landslide slip, Transactions of Nonferrous Metals Society of China, Vol. 23, No. 5, pp. 1459~1464.
59. Ziemer, R. R. (1981), The role of vegetation in the stability of forested slopes. Proceedings of the International Union of Forestry Research Organizations, Kyoto, Japan, XVII World Congress, pp. 297~308.